Inorg. Chem. **2004**, *43*, 7702–7708

Computational Modeling of Di-Transition-Metal-Substituted γ-Keggin Polyoxometalate Anions. Structural Refinement of the Protonated Divacant Lacunary Silicodecatungstate

Djamaladdin G. Musaev*[,1] and Keiji Morokuma

Cherry L. Emerson Center for Scientific Computation and Department of Chemistry, Emory University, 1515 Dickey Drive, Atlanta, Georgia 30322

Yurii V. Geletii and Craig L. Hill

Department of Chemistry, Emory University, 1515 Dickey Drive, Atlanta, Georgia 30322

Received July 14, 2004

The B3LYP density functional method has been validated for the di-Mn-substituted γ-Keggin polyoxometalate (POM) anion, $[(SiO_4)Mn^{III}_2(OH)_2W_{10}O_{32}]^{4-}$, and for the divacant lacunary silicodecatungastate, γ-$[(SiO_4)W_{10}O_{32}]^{8-}$. This approach was shown to adequately describe the geometries of $[(SiO_4)Mn^{III}_2(OH)_2W_{10}O_{32}]^{4-}$ and γ-$[(SiO_4)W_{10}O_{32}]^{8}$. Three different geometrical models, "full", "medium", and "small", for Mn_2-γ-Keggin have also been validated. It was shown that the medium $[(SiO_4)Mn^{III}_2(OH)_2W_6O_{24}H_8]^{4-}$ model, as well as small $[(SiO_4)Mn^{III}_2(OH)_2W_4O_{18}H_{10}]^{2-}$ model, preserves structural features of the full system, $[(SiO_4)Mn^{III}_2(OH)_2W_{10}O_{32}]^{4-}$. However, the small model distorts the charge distribution at the "active site" of the system and should be used with caution. The same computational approach was employed to elucidate the structure of the di-Fe-substituted γ-Keggin POM. The structure of the acidic (tetra-protonated form) of lacunary POM, γ-$[(SiO_4)W_{10}O_{32}H_4]^{4-}$, was shown to be γ-$[(SiO_4)W_{10}O_{28}(OH)_4]^{4-}$ with four terminal hydroxo ligands, rather than γ-$[(SiO_4)W_{10}O_{30}(H_2O)_2]^{4-}$ with two aqua and two oxo(terminal) ligands as reported by Mizuno and co-workers (*Science* **2003**, *300*, 964). The observed and calculated asymmetry in the W–O(terminal) bond distances of γ-$[(SiO_4)W_{10}O_{32}H_4]^{4-}$ is explained in terms of the existence of $O^1H^1\cdots O^2H^2$ and $O^4H^4\cdots O^3H^3$ hydrogen-bonding patterns in the γ-$[(SiO_4)W_{10}O_{28}(OH)_4]^{4-}$ structure.

I. Introduction

Metal oxide cluster anions (polyoxometalates, or POMs) are a large and rapidly growing class of inorganic compounds. Among many different types of POMs, Keggin-type heteropolyanions (generic formula $X^{n+}M_{12}O_{40}^{(8-n)-}$) are the best known and studied (see Chart 1).[1] Briefly, the Keggin structure consists of four M_3O_{13} groups bonded to each other at the corners of a tetrahedron surrounding the central heteroatom, X. Each of the four M_3O_{13} groups in this structure can be attached in one of two ways, which gives rise to five so-called "Baker−Figgis" (or cap rotation) isomers.[2] The α isomer is usually the most stable and the most abundant. The β, γ, δ, and ϵ isomers involve rotation of one, two, three, and four M_3O_{13} groups relative to the α isomer, respectively. The literature on fundamental properties and applications of polyoxometalates is quite substantial and growing very rapidly.[3] Recently, several reviews have been published on POM-containing nanostructures,[4] electronic and/or redox-active materials,[5] and homogeneous and heterogeneous catalysis systems.[6,7]

The stability and versatility of Keggin POMs, as well as the tunability of their size, charge, composition, and redox

* Corresponding author. E-mail: dmusaev@emory.edu. tel.: 1-404-727-2382.

(1) (a) Pope, M. T.; Muller, A. *Angew. Chem., Int. Ed. Engl.* **1991**, *30*, 34−48. (b) Coronado, E.; Gómez-García, C. J. *Chem. Rev.* **1998**, *98*, 273−296. (c) Klemperer, W. G.; Wall, C. G. *Chem. Rev.* **1998**, *98*, 297−306. (d) Kozhevnikov, I. V. *Chem. Rev.* **1998**, *98*, 171−198 and references therein.

(2) See: Anderson, T. M.; Hill, C. L. *Inorg. Chem.* **2002**, *41*, 4252−4258.

(3) Hill, C. L. Polyoxometalates: Reactivity. In *Comprehensive Coordination Chemistry II: Transition Metal Groups 3−6*; Wedd, A. G., Ed.; Elsevier Science: New York, 2004; Vol. 4, Chapter 4.11, pp 679−759.

(4) See: (a) Sanchez, C.; Soler-Illia, G. J. d. A. A.; Ribot, F.; Lalot, T.; Mayer, C. R.; Cabuil, V. *Chem. Mater.* **2001**, *13*, 3061−3083, (b) Clemente-Leon, M.; Coronado, E.; Delhaes, P.; Gomez-Garcia, C. J.; Mingotaud, C. *Adv. Mater.* **2001**, *13*, 574−577 and references therein.

10.1021/ic0490674 CCC: $27.50
Published on Web 10/29/2004

Chart 1. Structure of the Parent (Unsubstituted) Keggin POM in (A) Atom and (B) Polyhedral Notation[a]

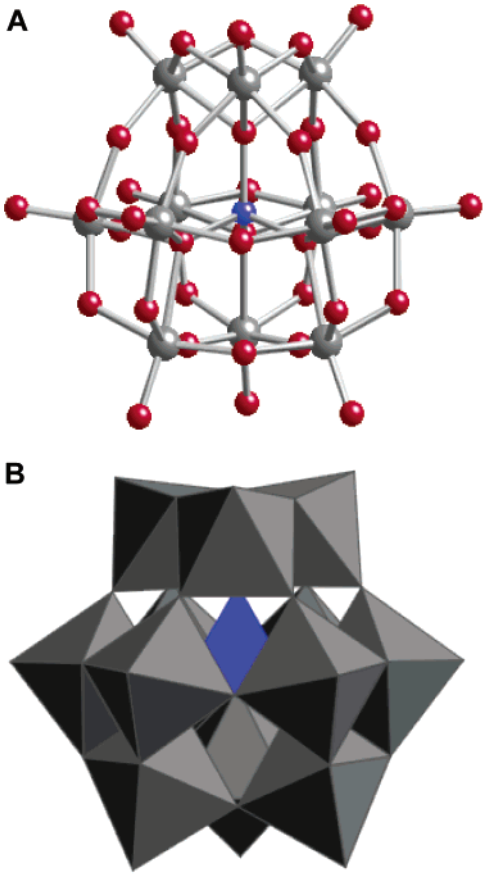

[a] The heteroatom, X, resides in the central tetrahedral cavity, and 12 metal atoms, M, most frequently W(VI) or Mo(VI), reside on the outside. All of the metal atoms in this dominant alpha (T_d) isomer are equivalent by symmetry.

properties, make them attractive for application in catalysis and other technologies. In fact, three of the four most important prototype catalysts in the scientific literature at present for homogeneous selective oxidation by O_2 alon (no sacrificial reductant required) are POM derivatives.[8−10]

Recently, derivatives of γ-Keggin POMs substituted by two d-electron-containing redox-active transition metals (with generic formula of $XM_2W_{10}O_{36}^{n-}$), reported to have remarkable catalytic activities in oxidation of different substrates (olefins, alkanes, and others) by O_2 and/or H_2O_2, have been attracting the interest of researchers.[8] Given that the design and realization of catalysts capable of such transformations has a significant industrial importance, fundamental properties of these compounds need comprehensive experimental and theoretical investigation. This paper addresses the theoretical modeling of γ-Keggin POMs substituted by two d-electron-containing redox-active transition metals, as well as lacunary (or defect) POMs; elucidates the geometry and electronic structure of some members of the POM structure family; and determines optimal theoretical approaches for investigation of their catalytic activities.

Keggin POMs have been the subject of several previous theoretical studies.[11] In general, these studies have demonstrated the applicability of the popular hybrid density functional approaches to study the geometries and electronic structures of these POMs. However, theoretical treatment of derivatives of γ-Keggin POMs substituted by two d-electron-containing redox-active transition metals is much more difficult because of the existence of multiple lower-lying electronic states. To our knowledge, such substituted POMs have never been the subject of theoretical studies. Nor have the structures and stabilities of lacunary POMs been studied theoretically before.

In this paper, we search for optimal theoretical approaches (both methods and models) to study the geometrical and electronic structures of di-transition-metal-substituted γ-Keggin POMs of the formula $[(SiO_4)M_2(OH)_2W_{10}O_{32}]^{4-}$, where M = Mn and Fe, as well as the lacunary POMs γ-$[(SiO_4)W_{10}O_{32}]^{8-}$ and γ-$[(SiO_4)W_{10}O_{32}H_4]^{4-}$.

II. Computation Procedure

In these calculations, we used the hybrid density functional B3LYP method, which combines the three-parameter exchange

(5) (a) Clemente-Leon, M.; Coronado, E.; Galan-Mascaros, J. R.; Gimenez-Saiz, C.; Gomez-Garcoa, C. J.; Martinez-Ferrero, E. *Synth. Met.* **2001**, *120*, 733−734. (b) Cheng, S.; Fernandez-Otero, T.; Coronado, E.; Gomez-Garcia, C. J.; Martinez-Ferrero, E. *J. Phys. Chem. B* **2002**, *106*, 7585−7591. (c) Ouahab, L. *Solid State Chem. Cryst. Chem.* **1998**, *2*, 369−380. (d) Coronado, E.; Mingotaud, C. *Adv. Mater.* **1999**, *11*, 869−872. (e) Yamase, T. *Chem. Rev.* **1998**, *98*, 307−326. (e) Keita, B.; Nadjo, L.; Contant, R. *J. Electroanal. Chem.* **1998**, *443*, 168−174. (f) Sadakane, M.; Steckhan, E. *Chem. Rev.* **1998**, *98*, 219−238. (g) Keita, B.; Nadjo, L. *Mater. Chem. Phys.* **1989**, *22*, 77−103. (h) Bond, A. M.; Way, D. M.; Wedd, A. G.; Compton, R. G.; Booth, J.; Eklund, J. C. *Inorg. Chem.* **1995**, *34*, 3378−3384.

(6) Reviews of catalysis by polyoxometalates: (a) Hill, C. L.; Prosser-McCartha, C. M. *Coord. Chem. Rev.* **1995**, *143*, 407−455. (b) Okuhara, T.; Mizuno, N.; Misono, M. *Adv. Catal.* **1996**, *41*, 113−252. (c) Mizuno, N.; Misono, M. *Chem. Rev.* **1998**, *98*, 199−218. (d) Kozhevnikov, I. V. *Chem. Rev.* **1998**, *98*, 171−198. (e) Neumann, R. *Prog. Inorg. Chem.* **1998**, *47*, 317−370. (f) Moffat, J. B. *Metal−Oxygen Clusters: The Surface and Catalytic Properties of Heteropoly Oxometalates, Fundamental and Applied Catalysis*; Kluwer Academic/Plenum Publishers: New York, 2001; Vol. 9. (g) Kozhevnikov, I. V. *Catalysis by Polyoxometalates*; Wiley: Chichester, U.K., 2002; Vol. 2.

(7) (a) Weinstock, I. A.; Barbuzzi, E. M. G.; Wemple, M. W.; Cowan, J. J.; Reiner, R. S.; Sonnen, D. M.; Heintz, R. A.; Bond, J. S.; Hill, C. L. *Nature* **2001**, *414*, 191−195. (b) Grigoriev, V. A.; Hill, C. L.; Weinstock, I. A. *J. Am. Chem. Soc.* **2000**, *122*, 3544−3545. (c) Grigoriev, V. A.; Cheng, D.; Hill, C. L.; Weinstock, I. A. *J. Am. Chem. Soc.* **2001**, *123*, 5292−5307. (d) Weinstock, I. A. *Chem. Rev.* **1998**, *98*, 113−170.

(8) Nishiyama, Y.; Nakagawa, Y.; Mizuno, N. *Angew. Chem., Int. Ed.* **2001**, *40*, 3639−3641.

(9) (a) Neumann, R.; Dahan, M. *Nature* **1997**, *388*, 353−355. (b) Neumann, R.; Dahan, M. *J. Am. Chem. Soc.* **1998**, *120*, 11969−11976.

(10) Okun, N. M.; Anderson, T. M.; Hill, C. L. *J. Am. Chem. Soc.* **2003**, *125*, 3194−3195.

(11) (a) Kempf, J. Y.; Rohmer, M. M.; Poblet, J. M.; Bo, C.; Benard, M. *J. Am. Chem. Soc.* **1992**, *114*, 1136−1146. (b) Rohmer, M. M.; Benard, M. *J. Am. Chem. Soc.* **1994**, *116*, 6959−6960. (c) Rohmer, M. M.; Devemy, R.; Wiest, M.; Benard, M. *J. Am. Chem. Soc.* **1996**, *118*, 13007−13014. (d) Rohmer, M. M.; Benard, M.; Blaudeau, J. P.; Maestre, J. M.; Poblet, J. M. *Coord. Chem. Rev.* **1998**, *178−180*, 1019−1049. (e) Bridgeman, A. J. *Chem. Phys.* **2003**, *287*, 55−69. (f) Bridgeman, A. J.; Cavigliasso, G. *Chem. Phys.* **2002**, *279*, 143−149. (g) Maestre, J. M.; Lopez, X.; Bo, C.; Daul, C.; Poblet, J. M. *Inorg. Chem.* **2002**, *41*, 1883−1888. (h) Bridgeman, A. J.; Cavigliasso, G. *Inorg. Chem.* **2002**, *41*, 1761−1770. (l) Bridgeman, A. J.; Cavigliasso, G. *J. Phys. Chem. A* **2002**, *106*, 6114−6120. (m) Lopez, X.; Bo, C.; Poblet, J. M. *J. Am. Chem. Soc.* **2002**, *124*, 12574−12582. (n) Lopez, X.; Maestre, J. M.; Bo, C.; Poblet, J.-M. *J. Am. Chem. Soc.* **2001**, *123*, 9571−9576. (o) Duclusaud, H.; Borshch, S. A. *J. Am. Chem. Soc.* **2001**, *123*, 2825−2829. (p) Maestre, J. M.; Lopez, X.; Bo, C.; Poblet, J.-M.; Casañ-Pastor, N. *J. Am. Chem. Soc.* **2001**, *123*, 3749−3758. (q) Duclusaud, H.; Borshch, S. A. *Inorg. Chem.* **1999**, *38*, 3491−3493.

Chart 2. Schematic Representation of Geometrical Models of Di-Transition-Metal-Substituted γ-Keggin POMs and the Atom Assignments Used

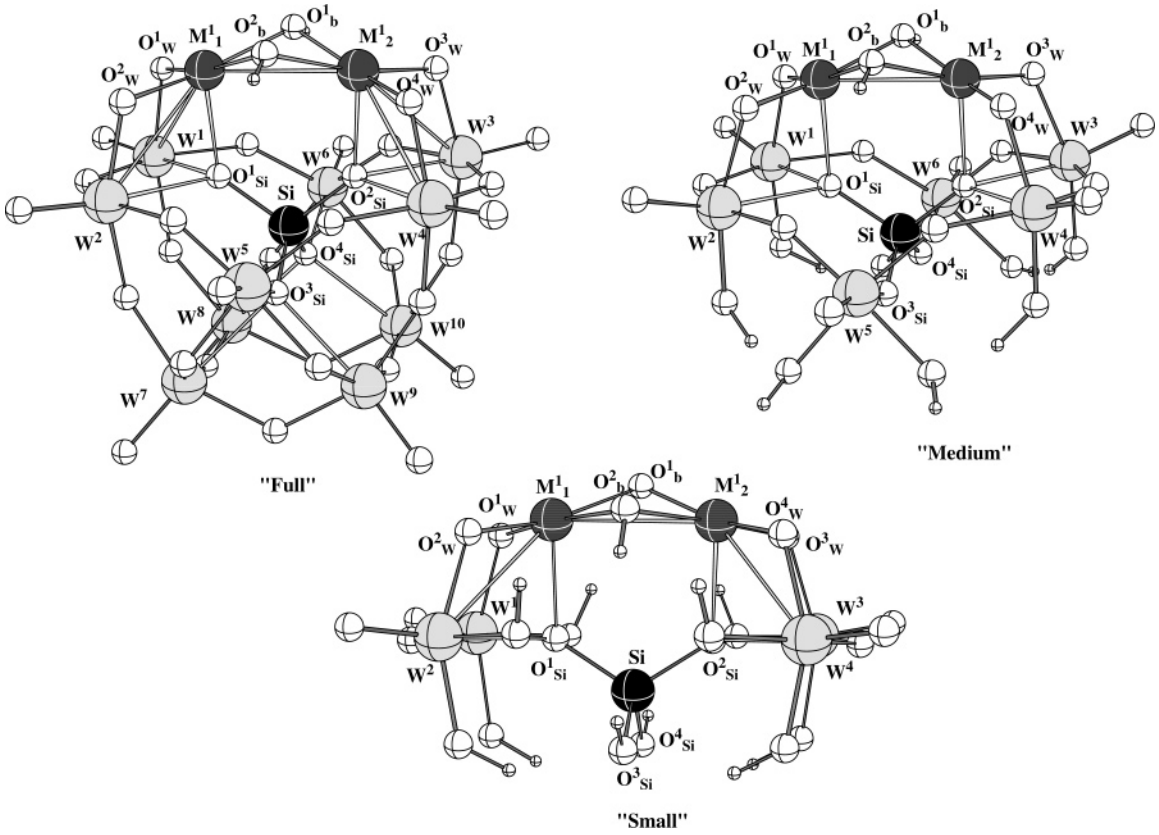

functional of Becke (B3)[12] with the Lee−Yang−Parr (LYP) correlation functional[13] and the Lanl2dz basis set[14] augmented with the polarization d-function [with $\alpha_d(Si) = 0.55$] on the Si atom [this basis set will be referred to as Lanl2dz + d(Si)]. Geometries of all structures were optimized with the analytical gradient method without symmetry constraints. All calculations were performed by the quantum chemical package Gaussian 03.[15]

We used three different structural models, as shown in Chart 2, for di-transition-metal-substituted γ-Keggin POMs (M_2-γ-Keggin) based on the following general criteria: (1) Each model should preserve the cage structure of the entire POM; (2) any modification to the model should not alter the oxidation states of the substituted transition metal atoms M, tungsten atoms in the main frame, or heteroatom Si; and (3) modeling should not significantly affect the ligand environment of the central Si atom, or in other words, the Si atom should have four single Si−O bonds.

Therefore, the "full" model contains all atoms, except two terminal water molecules coordinated to two transition metals M_2. Preliminary calculations showed that these terminal water molecules are weakly bound to M_2 and can be excluded. The general formula of this full model is $[(SiO_4)M^{III}_2(OH)_2W_{10}O_{32}]^{4-}$. Because this model is very large and requires excessive computational resources in studying catalytic mechanisms, we decided to validate two smaller models. The "medium" model simplifies the full model by eliminating four of the tungsten atoms (W^7, W^8, W^9, and W^{10}; see Chart 2) with the associated oxygen ligands and terminating the produced dangling O−X bonds by H atoms. This medium model of POM has the formula of $[(SiO_4)M^{III}_2(OH)_2W_6O_{24}H_8]^{4-}$. The "small" model further excludes the W^5 and W^6 centers with the associated oxygen atoms from the medium model, and similarly, the additional dangling O−X bonds are terminated by H atoms. The formula of this small model is $[(SiO_4)M^{III}_2(OH)_2W_4O_{18}H_{10}]^{2-}$. As seen from this formula, the total charge of the small model is −2, compared with −4 for medium and full models. This modification to the total charge of the system was introduced to keep the same ligand environment of the heteroatom, i.e., the Si atom should have four single Si−O bonds.

To study the lacunary POM, we propose three possible structures given in Chart 3. The first proposed structure deals with the generic lacunary POM with formula γ-$[(SiO_4)W_{10}O_{32}]^{8-}$ that has four terminal oxo ligands. This complex has been experimentally characterized by Herve and co-workers.[16] To validate the method used in this paper, we calculated the geometrical and electronic

(12) (a) Becke, A. D. *Phys. Rev. A* **1988**, *38*, 3098−3107, (b) Becke, A. D. *J. Chem. Soc.* **1993**, *98*, 1372−1380.
(13) Lee, C.; Yang, W.; Parr, R. G. *Phys. Rev. B* **1988**, *37*, 785−789.
(14) (a) Hay, P. J.; Wadt, *J. Chem. Phys.* **1985**, *82*, 299−310. (b) Hay, P. J.; Wadt, W. R. *J. Chem. Phys.* **1985**, *82*, 270−283. (c) Wadt, W. R.; Hay, P. J. *J. Chem. Phys.* **1985**, *82*, 284−298.
(15) Frisch, M. J.; Trucks, G. W.; Schlegel, H. B.; Scuseria, G. E.; Robb, M. A.; Cheeseman, J. R.; Montgomery, J. A., Jr.; Vreven, T.; Kudin, K. N.; Burant, J. C.; Millam, J. M.; Iyengar, S. S.; Tomasi, J.; Barone, V.; Mennucci, B.; Cossi, M.; Scalmani, G.; Rega, N.; Petersson, G. A.; Nakatsuji, H.; Hada, M.; Ehara, M.; Toyota, K.; Fukuda, R.; Hasegawa, J.; Ishida, M.; Nakajima, T.; Honda, Y.; Kitao, O.; Nakai, H.; Klene, M.; Li, X.; Knox, J. E.; Hratchian, H. P.; Cross, J. B.; Adamo, C.; Jaramillo, J.; Gomperts, R.; Stratmann, R. E.; Yazyev, O.; Austin, A. J.; Cammi, R.; Pomelli, C.; Ochterski, J. W.; Ayala, P. Y.; Morokuma, K.; Voth, G. A.; Salvador, P.; Dannenberg, J. J.; Zakrzewski, V. G.; Dapprich, S.; Daniels, A. D.; Strain, M. C.; Farkas, O.; Malick, D. K.; Rabuck, A. D.; Raghavachari, K.; Foresman, J. B.; Ortiz, J. V.; Cui, Q.; Baboul, A. G.; Clifford, S.; Cioslowski, J.; Stefanov, B. B.; Liu, G.; Liashenko, A.; Piskorz, P.; Komaromi, I.; Martin, R. L.; Fox, D. J.; Keith, T.; Al-Laham, M. A.; Peng, C. Y.; Nanayakkara, A.; Challacombe, M.; Gill, P. M. W.; Johnson, B.; Chen, W.; Wong, M. W.; Gonzalez, C.; Pople, J. A. *Gaussian 03*; Gaussian, Inc.: Pittsburgh, PA, 2003.
(16) Canny, J.; Tézé, A.; Thouvenot, R.; Hervé, G. *Inorg. Chem.* **1986**, *25*, 2114−2119.

Chart 3. Schematic Representation of the Lacunar POMs and the Atom Assignments Used

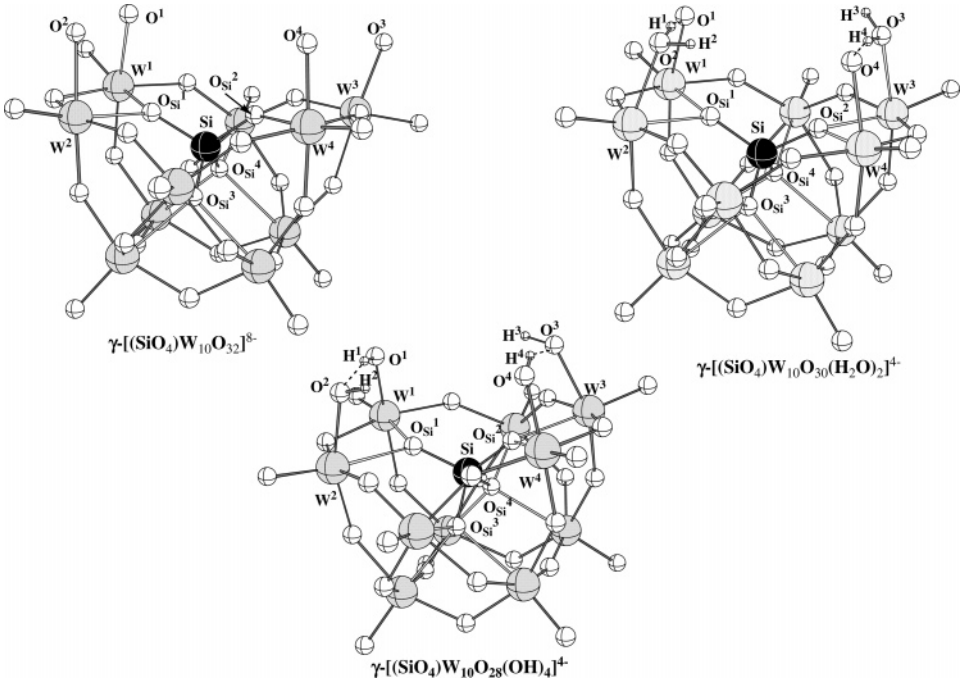

structures of this generic lacunary POM and compared these results with the available experimental values. The second and third proposed structures for lacunary POM are dictated by the recent report of Mizuno and co-workers[17] and deal with the tetraprotonated form of this anion, γ-$[(SiO_4)W_{10}O_{32}H_4]^{4-}$. On the basis of X-ray data, Mizuno et al. concluded that two of the four oxo ligands in this system are doubly protonated and the resultant water molecules are coordinated to the W^2 and W^3 atoms. However, we believe that the assignment of the positions of these four protons in this system needs additional investigation. Indeed, it is worth clarifying why the four protons coordinate to only two oxo ligands while the two other oxo ligands remain coordinatively unsaturated. In the other words, can the structure involving four hydroxo group be ruled out? To answer these questions, we calculated the energies and geometries of the complexes γ-$[(SiO_4)W_{10}O_{30}(H_2O)_2]^{4-}$ and γ-$[(SiO_4)W_{10}O_{28}(OH)_4]^{4-}$ (Chart 3).

This paper is organized into four parts. In section III.A we discuss the geometries, atomic spin densities, and Mulliken charges of the Mn_2-γ-Keggin POM. We compare our findings with the available experimental data and validate the methods and models used in these studies. In section III.B, we apply the same approaches to the Fe_2-γ-Keggin POM. In section III.C, we elucidate the geometrical and electronic structures of the lacunary POM and compare our results with the available experiments. In section IV, we summarize our findings.

III. Results and Discussions

A. Mn_2-γ-Keggin POM: $[(SiO_4)Mn^{III}_2(OH)_2W_{10}O_{32}]^{4-}$. Manganese-substituted polyoxotungstates has been the subject of intensive experimental studies, including X-ray analysis,[18] partly inspired by the role of such moieties in redox-active enzymes such as manganese catalase. Therefore, these compounds are among the best systems to use in evaluating and validating our theoretical approach and models.

It has been shown that mono- and trimanganese heteropolyanions exhibit significant catalytic activity in epoxidation of alkenes.[18] Experimental studies[18d] of $[(CH_3)_3(C_6H_5)N]_4$-$[(SiO_4)Mn_2W_{10}O_{36}H_6]\cdot 2CH_3CN\cdot H_2O$ (**1**) show that this anion has the γ-Keggin structure with near-C_{2v} symmetry, where the two Mn cations occupy adjacent, edge-shared octahedra with bridging hydroxo and terminal aqua ligands and are separated by 2.93 Å. Magnetic susceptibility studies combined with X-ray crystallography studies showed that the Mn centers are in their high-valent Mn^{III} states in this compound and are antiferromagnetically coupled with coupling constant of $J = -17$ cm^{-1}.

Because the interaction of the terminal water molecules with Mn centers is very weak and the reported antiferromagnetic coupling constant in anion **1** is relatively small, below, we report the calculated geometrical and electronic structures of the ferromagnetically coupled $[(SiO_4)Mn_2(OH)_2W_{10}O_{32}]^{4-}$ complex. In Table 1, we present the important bond distances optimized at the spin-unrestricted level of theory with $2M_S + 1 = 9$ for the full, medium, and small models and compare these results with the experimental values. All optimizations converged to nearly C_{2v} structures. As seen from this table, the calculated bond distances for the full model are in excellent agreement with the experimental values. The largest discrepancy between the calculated and experimental data is about 0.1 Å, corresponding to the nonrigid (very weak) W−O_{Si} and Mn−O_{Si} bonds. These

(17) Kamata, K.; Yonehara, K.; Sumida, Y.; Yamaguchi, K.; Hikichi, S. Mizuno, N. *Science* **2003**, *300*, 964−966.

(18) Representative catalytic studies of manganese-containing POMs include: (a) Hill, C. L.; Brown, R. B. *J. Am. Chem. Soc.* **1986**, *108*, 536−538. (b) Neumann, R.; Gara, M. *J. Am. Chem. Soc.* **1994**, *116*, 5509−5510. (c) Neumann, R.; Gara, M. *J. Am. Chem. Soc.* **1995**, *117*, 5066−5074. (d) Zhang, X.-Y.; O'Connor, C. J.; Jameson, G. B.; Pope, M. T. *Inorg. Chem.* **1996**, *35*, 30−34. (e) Neumann, R.; Khenkin, A. M. *Chem. Commun.* **1998**, 1967−1968. (f) Ben-Daniel, R.; Weiner, L.; Neumann, R. *J. Am. Chem. Soc.* **2002**, *124*, 8788−8789. (g) Adam, W.; Alsters, P. L.; Neumann, R.; Saha-Moller, C. R.; Sloboda-Rozner, D.; Zhang, R. *Synlett* **2002**, 2011−2014. (h) Adam, W.; Herold, M.; Hill, C. L.; Saha-Möller, C. R. *Eur. J. Org. Chem.* **2002**, 941−946.

Table 1. Optimized Important Bond Distances (in Å) of the Mn_2-γ-Keggin POM, $[(SiO)_4Mn^{III}_2(OH)_2W_{10}O_{32}]^{4-}$, for the $^9A_1$ Electronic State Calculated Using Full, Medium, and Small Geometrical Models[a]

atoms	full	medium	small	expt
Mn^1-Mn^2	2.924	2.896	2.988	2.935
$Mn^1-O_b{}^1$	1.957	1.956	1.968	1.923(14)−1.967(14)
$Mn^1-O_{Si}{}^1$	2.207	2.197	2.163	2.306(14)−2.328(12)
$Mn^1-O_W{}^1$	1.847	1.841	1.858	1.863(14)−1.902(13)
$Si-O_{Si}{}^1$	1.637	1.664	1.622	1.632(13)−1.658(14)
$Si-O_{Si}{}^3$	1.638	1.616	1.656	1.632(13)−1.658(14)
$W^1-O_W{}^1$	1.908	1.914	1.908	1.879(12)−2.00(2)
$W^1-O_{Si}{}^1$	2.400	2.453	2.519	2.276(12)−2.340(14)
$W^5-O_{Si}{}^3$	2.380	1.985	−	

[a] The calculations, which were performed without any geometry constraints, converge to the structure with the C_{2v} symmetry. Therefore, in this table, we present only important symmetric bond distances.

Table 2. Atomic Spin Densities (in e) and Mulliken Atomic Charges (in e) of $[(SiO)_4Mn^{III}_2(OH)_2W_{10}O_{32}]^{4-}$, in the $^9A_1$ Electronic State Calculated Using Full, Medium, and Small Geometrical Models[a]

	full		medium		small	
atom	spin	charge	spin	charge	spin	charge
Mn^1	3.79	0.98	3.77	0.96	3.79	1.02
Mn^2	3.79	0.98	3.77	0.96	3.79	1.02
$O_b{}^1$	0.01	−0.30	0.01	−0.30	0.01	−0.36
Si	0.00	1.84	0.00	1.59	0.00	1.40
$O_{Si}{}^1$	0.07	−0.86	0.08	−0.84	0.08	−0.82
$O_{Si}{}^3$	0.00	−0.84	0.00	−0.74	0.00	−0.32
$O^3{}_W$	0.05	−0.66	0.05	−0.55	0.04	−0.48
W^1		1.70		1.63		1.55
W^5		1.65		1.39		
W^7		1.73		−		
total	7.94	−4.00	7.92	−4.00	7.92	−2.00
SiO_4		−1.56		−1.57		−0.88

[a] See footnote to Table 1.

results validate the application of the B3LYP/Lanl2dz +d(Si) method to the Mn_2-γ-Keggin POM.

Upon going from the full model to the medium and small models, the cage structure of POM is preserved, and all geometrical parameters in the vicinity of the active centers (Mn atoms) are described appropriately. However, the $W^5-O_{Si}{}^3$ bond distance shortens significantly, to 0.395 Å, upon going from the full to the medium model, which is a result of the lack of $W^7-O_{Si}{}^3$ and $W^9-O_{Si}{}^3$ interactions in the medium model compared to full model. These results allow us to conclude that, like the density functional method used, the proposed models for the Mn_2-γ-Keggin POMs are valid for investigation of the geometries of the M_2-γ-Keggin POMs.

As seen in Table 2, where we present the calculated atomic spin densities and Mulliken charges, almost four (about 3.77−3.79) unpaired electrons are located on the Mn centers, indicating that they are in their high-valent Mn^{III} states regardless of the model used. This conclusion is consistent with experimental assignment of high-valent Mn^{III} centers in anion **1**. However, one should again note that, in our calculations, we assumed the antiferromagnetic coupling between the Mn centers to be very small. As a consequence, only the ferromagnetic state was calculated.

As seen in Table 2, the calculated Mulliken charges of the Mn and O_b atoms are very similar in the full, medium, and small models. In contrast, the charges of the Si and O atoms in the SiO_4 unit, as well as the O atoms bridging the Mn and W centers, are quite different for different models, especially for the small model. Therefore, the small model should be used with considerable caution to study the catalytic activity of these species.

Table 3. Calculated Important Bond Distances (in Å) and Relative Energies (in kcal/mol) of the Lower-Lying $^{11}A'$ and $^7A'$ Electronic States of the Fe_2-γ-Keggin POM, $[(SiO_4)Fe_2(OH)_2W_{10}O_{32}]^{4-}$ Calculated Using Full, Medium, and Small Geometrical Models[a]

	full		medium		small
atoms	$^{11}A'$	$^7A'$	$^{11}A'$	$^7A'$	$^{11}A'$
Fe^1-Fe^2	2.969	2.878	2.938	2.832	2.978
$Fe^1-O_b{}^1$	2.010	1.950	2.015	1.939	2.014
$Fe^1-O_{Si}{}^1$	2.046	2.185	2.017	2.188	1.921
$Fe^1-O_W{}^1$	1.903	1.858	1.899	1.822	2.081
$Fe^1-O_W{}^2$	1.902	1.802	1.899	1.822	2.081
$Si-O_{Si}{}^1$	1.647	1.637	1.669	1.664	1.666
$Si-O_{Si}{}^3$	1.629	1.637	1.604	1.616	1.725
$W^1-O_W{}^1$	1.891	1.895	1.896	1.918	1.829
$W^2-O_W{}^2$	1.899	1.928	1.896	1.918	1.829
$W^1-O_{Si}{}^1$	2.463	2.386	2.524	2.432	4.757
$W^5-O_{Si}{}^3$	2.424	2.381	1.998	1.985	−
ΔE	0.0	5.8	0.0	7.2	0.0

[a] The calculations, which were performed without any geometry constraints, converge to the structure with C_s symmetry. Therefore, in this table, we present only important symmetric bond distances.

Summarizing, the studies of the Mn_2-γ-Keggin POMs show that (a) hybrid density functional method B3LYP adequately describes the geometries of M_2-γ-Keggin POMs and (b) all three models preserve the cage structure of Mn_2-γ-Keggin POM and could be applied to further studies of these species. In contrast, the small model does not describe the charge distribution of the POMs adequately.

B. Fe_2-γ-Keggin POM: $[(SiO_4)Fe_2(OH)_2W_{10}O_{32}]^{4-}$. With validation of the theoretical method and geometrical modeling scheme for the Mn_2-γ-Keggin POM, we now address the geometrical and electronic structures of the Fe_2-γ-Keggin POM. This POM was reported to be an excellent catalyst for hydrocarbon oxidation based, in part, on the resemblance of its "active site" to that of methane monooxygenase (MMO).[19] Furthermore, Mizuno and co-workers recently reported that the Fe_2-γ-Keggin POM efficiently catalyzes the epoxidation of alkenes with molecular oxygen.[8] However, the geometrical and electronic structures of this important complex remain unclear.

Importantly, optimization of the geometries of three different models (full, medium, and small) for this POM without any symmetry constraints resulted in structures with nearly C_{2v} or C_s symmetry. Therefore, for simplicity, in Table 3, we present only symmetric bond distances for lower-lying electronic states with multiplicities of $2M_S + 1 = 11$ (10 spins) and 7 (6 spins) for these model compounds. To evaluate the effect of the full, medium, and small models of

(19) (a) Rosenzweig, A. C.; Nordlund, P.; Takahara, P. M.; Frederick, C. A.; Lippard, S. J. *Chem. Biol.* **1995**, *2*, 409−418. (b) Whittington, D. A.; Lippard, S. J. *J. Am. Chem. Soc.* **2001**, *123*, 827−838. (c) Solomon, E.; Brunold, T. C.; Davis, M. I.; Kemsley, J. N.; Lee, S.-K.; Lehnert, N.; Neese, F.; Skulan, A. J.; Yang, Y.-S.; Zhou, J. *Chem. Rev.* **2000**, *100*, 235−349. (d) Merkx, M.; Kopp, D. A.; Sazinsky, M. H.; Blazyk, J. L.; Muller, J.; Lippard, S. J. *Angew. Chem., Int. Ed.* **2001**, *40*, 2782−2807.

the Fe_2-γ-Keggin POM on the energy of the lower-lying electronic states, we also provide the relative energies of the $^{11}A'$ and $^{7}A'$ electronic states calculated at the B3LYP level. However, it has to be noted that the calculated energy gap between the lower-lying electronic states of this system could change upon use of different density functionals (such as BP86, BLYP, etc.). The accurate calculations of the energy gap between the various lower-lying electronic states of the M_2-γ-Keggin POMs requires sophisticated approaches such as the complete-active-space-self-consistent-field (CASSCF), multireference-single-double-CI (MR-SDCI), and coupled-cluster [CCSD(T)] methods. Unfortunately, the application these sophisticated methods on large systems such as the Fe_2-γ-Keggin POM is not technically feasible, and therefore, these type of calculations are not performed in this study.

As seen in Table 3 for the full model system, the state with $2M_S + 1 = 11$, $^{11}A'$, is slightly (5.8 kcal/mol) more stable than that with $2M_S + 1 = 7$, $^{7}A'$. The calculated Fe−Fe, Fe−O_b^1, Fe−O_W^1, and Fe−O_W^2 distances are 2.969, 2.010, 1.903, and 1.902 Å, respectively, for the $^{11}A'$ state. These values are slightly smaller for $^{7}A'$ state: 2.878, 1.950, 1.858, and 1.802 Å, respectively. Meanwhile, the calculated $Fe^1-O_{Si}^1$ (or $Fe^2-O_{Si}^2$ distance, which is not given in the table) is larger for $^{7}A'$ than for $^{11}A'$: 2.185 vs 2.046 Å. These bond distances indicate that the Fe_2O_2 unit of the system becomes more compact upon going from $^{11}A'$ to $^{7}A'$. Other geometrical parameters change only slightly. Reducing the number of atoms included in the calculations in going from the full to the medium model does not affect the above conclusions. Comparison of the calculated geometrical parameters and relative energies of the lower-lying states for the full and medium models shows the applicability of the medium model to the study of the Fe_2-γ-Keggin POM.

Again, however, the results obtained for the small model are not encouraging. At first, optimization of the structure of the small model significantly destroys the cage structure of the POM. As seen in Table 3, the $W^1-O_{Si}^1$ (as well as $W^2-O_{Si}^1$, $W^3-O_{Si}^2$, and $W^4-O_{Si}^2$, which are not presented in Table 3) distance becomes very large, 4.757Å, and in fact, the W_2O_5 units are flipped up (away from SiO_4 unit). Thus, the use of the small model in the future should be avoided (or undertaken with great caution).

In Table 4, we show the calculated atomic spin densities and Mulliken charges for the presented models of the Fe_2-γ-Keggin POM. Clearly, the spin and charge distributions are very similar for the full and medium models. Almost four and three unpaired electrons are located on each of the Fe centers for the $^{11}A'$ and $^{7}A'$ states, respectively. Two more electrons for each state are distributed primarily among the O_b and O_W centers (located between the W and Fe centers). In the medium model, the SiO_4 unit has more negative charge than in the full model, mainly because the Si center is less positively charged in the medium (1.58 e) than in the full (1.85 e) model. We will not discuss the charge and spin distributions for the small model.

C. Lacunary POM: γ-$[(SiO_4)W_{10}O_{32}]^{8-}$, γ-$[(SiO_4)W_{10}O_{30}(H_2O)_2]^{4-}$, and γ-$[(SiO_4)W_{10}O_{28}(OH)_4]^{4-}$. The optimized geometries of the lacunary POMs (see Chart 3) are given in Table 5. Initially, our calculations show that all three compounds have a singlet ground electronic state. As seen from the Table 5, the important calculated and experimental bond distances for γ-$[(SiO_4)W_{10}O_{32}]^{8-}$ are in very good agreement, which, once again, confirms the applicability of the B3LYP/lanl2dz+d(Si) approach to POMs.

As mentioned above, the interest in γ-$[(SiO_4)W_{10}O_{30}(H_2O)_2]^{4-}$ and γ-$[(SiO_4)W_{10}O_{28}(HO)_4]^{4-}$ is dictated by the recent report of Mizuno and co-workers[17] on the structure and catalytic activity of the tetra-protonated form of the lacunary POM, γ-$[(SiO_4)W_{10}O_{32}H_4]^{4-}$, **2**. Briefly, it was shown that the catalytic activity of this lacunary POM appears to depend on the pH at which the POM was prepared; the catalyst **2** prepared at pH 2 exhibits the highest

Table 4. Atomic Spin Densities (in e) and Mulliken Charges (in e) of the Fe_2-γ-Keggin POM in Its Two Lowest Electronic States Calculated Using Full, Medium, and Small Geometrical Models[a]

	full				medium				small	
	spin		charge		spin		charge		spin	charge
atom	$^{11}A'$	$^{7}A'$	$^{11}A'$	$^{7}A'$	$^{11}A'$	$^{7}A'$	$^{11}A'$	$^{7}A'$	$^{11}A'$	$^{11}A'$
Fe^1	4.06	2.78	0.97	0.81	3.99	3.13	1.02	0.83	3.97	1.00
Fe^2	4.06	2.78	0.97	0.81	3.99	3.13	1.02	0.83	3.97	1.00
O_b^1	0.25	−0.05	−0.32	−0.22	0.26	−0.54	−0.42	−0.41	0.21	−0.45
Si	0.15	0.00	1.85	1.85	0.00	0.00	1.54	1.58	0.01	1.60
O_{Si}^1	0.07	0.08	−0.86	−0.85	0.18	0.13	−0.87	−0.86	0.18	−0.91
O_{Si}^3	0.01	0.00	−0.82	−0.83	0.01	0.01	−0.75	−0.75	0.01	−0.47
O_W^1	0.26	0.00	−0.66	−0.62	0.25	0.13	−0.70	−0.64	0.10	−0.71
O_W^2	0.26	0.00	−0.66	−0.63	0.25	0.13	−0.70	−0.64	0.10	−0.71
W^1	−0.02	−0.01	1.72	1.70	−0.02	−0.01	1.67	1.66	0.23	1.77
W^5	0.00	0.00	1.64	1.72	0.00	0.00	1.45	1.45		
W^7	0.00	0.00	1.73	1.73						
Total			−4.00	−4.00			−4.00	−4.00		−2.00
SiO_4			−1.51	−1.53			−1.70	−1.64		−1.16

[a] See footnote to Table 3.

Table 5. Calculated Experimental Values of Important Bond Distances (in Å) of the Lacunary POMs γ-$[(SiO_4)W_{10}O_{32}]^{8-}$ and γ-$[(SiO_4)W_{10}O_{32}H_4]^{4-}$

	γ-$[(SiO_4)W_{10}O_{32}]^{8-}$		γ-$[(SiO_4)W_{10}O_{32}H_4]^{4-}$ calcd		
atoms	calcd	expt	Lac_2(H_2O)[a]	Lac_4(OH)[b]	expt
W^1-O^1	1.781	1.79(4)	1.799	1.906	∼1.72
W^2-O^2	1.781	1.77(4)	2.231	2.026	2.16(1)
W^3-O^3	1.781	1.72(6)	2.230	2.026	2.14(1)
W^4-O^4	1.781	1.70(5)	1.811	1.906	∼1.72
$W^1-O_{Si}^1$	2.313	2.21(5)	2.302	2.265	
$W^2-O_{Si}^1$	2.310	2.27(5)	2.237	2.289	
$W^3-O_{Si}^2$	2.313	2.34(4)	2.351	2.265	
$W^4-O_{Si}^2$	2.312	2.27(4)	2.350	2.265	
$Si-O_{Si}^1$	1.643	1.59(5)	1.617	1.616	
$Si-O_{Si}^2$	1.643	1.54(5)	1.617	1.616	
$Si-O_{Si}^3$	1.673	1.68(4)	1.649	1.654	
$Si-O_{Si}^3$	1.673	1.68(4)	1.649	1.654	
O^1-H^1			1.534	1.013	
O^2-H^1			1.044	1.696	
O^3-H^4			1.059	1.695	
O^4-H^4			1.469	1.014	
O^1-H^3			3.911	4.152	
O^3-H^3			0.982	0.979	
O^2-H^2			0.980	0.979	
O^4-H^2			3.978	4.152	
O^1-O^2	3.592		2.550	2.655	
O^1-O^3	5.594		5.037	5.010	
O^3-O^4	3.594		2.492	2.655	
O^2-O^4	5.601		4.868	5.010	

[a] γ-$[(SiO_4)W_{10}O_{30}(H_2O)_2]^{4-}$. $\Delta E = 0.0$. [b] γ-$[(SiO_4)W_{10}O_{28}(OH)_4]^{4-}$. $\Delta E = -8.0$.

activity. On the basis of X-ray analysis, the structure of **2** was formulated as γ-$[(SiO_4)W_{10}O_{30}(H_2O)_2]$,$^{4-}$ with two terminal aqua ligands. This conclusion was made on the basis of the observed asymmetry of the W−O(terminal) bond distances. Two W−O(terminal) bonds were found to be noticeably longer than other two: W^2-O^2 and W^3-O^3 were 2.16(1) and 2.14(1) Å, respectively, whereas W^1-O^1 and W^4-O^4 were in the range of 1.69(1)−1.75 (1) Å (Chart 3).

However, the structural assignment of the four protons in this system needs additional investigation to elucidate the question: why do all four protons coordinate to only two oxo ligands, while the other two oxo ligands remain coordinatively unprotonated? This is certainly counterintuitive according to simple Brønsted acidity arguments. To address this conundrum, we calculated the energies and geometries of the complexes γ-$[(SiO_4)W_{10}O_{30}(H_2O)_2]^{4-}$ and γ-$[(SiO_4)W_{10}O_{28}(OH)_4]^{4-}$.

As can be seen in Table 5, both structures have two short and two long W−O(terminal) bonds. In the structure γ-$[(SiO_4)W_{10}O_{30}(H_2O)_2]^{4-}$, the W^1-O^1 and W^4-O^4 bond distances (W−oxo bonds) are found to be 1.799 and 1.881 Å, respectively, while the W^2-O^2 and W^3-O^3 bond distances (W−aqua bonds) are significantly longer at 2.231 and 2.230 Å. Furthermore, the terminal water molecules are hydrogen bonded to the oxo ligands (O^1 and O^4); the calculated O^2-H^1 and $O^1\cdots H^1$ bond distances are 1.044 and 1.534 Å, respectively, while the O^3-H^4 and $O^4\cdots H^4$ bonds are 1.059 and 1.469 Å, respectively. These data, in general, are consistent with the X-ray data of Mizuno and co-workers.[17]

However, the γ-$[(SiO_4)W_{10}O_{28}(OH)_4]^{4-}$ structure with four terminal hydroxo ligands also has two short and two long W−O distances, although the difference between the long and short W−O distances is much smaller than that in γ-$[(SiO_4)W_{10}O_{30}(H_2O)_2]^{4-}$. Indeed, for γ-$[(SiO_4)W_{10}O_{28}(OH)_4]^{4-}$, the short W^1-O^1 and W^4-O^4 bond distances are 1.906 and 1.906 Å, while the long W^2-O^2 and W^3-O^3 bond distances are 2.026 and 2.026 Å. Furthermore, the difference in the calculated W−OH(terminal) bonds is result of the existing H-bonding patterns; the $O^1H^1\cdots O^2H^2$ and $O^4H^4\cdots O^3H^3$ hydrogen-bonding distances are 1.696 and 1.695Å, respectively. Because O^1-O^3 and O^2-O^4 distances are very long, 5.010 and 5.010 Å, respectively, there is no H-bonding between the O^2H^2/O^4H^4 and O^3H^3/O^1H^1 pairs. Thus, both the structure γ-$[(SiO_4)W_{10}O_{30}(H_2O)_2]^{4-}$ and the structure γ-$[(SiO_4)W_{10}O_{28}(OH)_4]^{4-}$ have two short and two long W−O(terminal) bonds. In short, the calculated (and observed) asymmetry in W−O(terminal) bond distances is not conclusive for formulating the structure of γ-$[(SiO_4)W_{10}O_{32}H_4]^{4-}$, **2**.

In this situation, we have to consider the relative energies of the two structures. Calculations show that γ-$[(SiO_4)W_{10}O_{28}(OH)_4]^{4-}$ with four terminal hydroxo ligands is about 8.0 kcal/mol more stable than γ-$[(SiO_4)W_{10}O_{30}(H_2O)_2]^{4-}$ with two aqua and two oxo(terminal) ligands. Therefore, we conclude that (a) the structure of γ-$[(SiO_4)W_{10}O_{32}H_4]^{4-}$, **2**, should be formulated as γ-$[(SiO_4)W_{10}O_{28}(OH)_4]^{4-}$, with four terminal hydroxo ligands, and (b) the asymmetry in the W−OH bond lengths is a result of existence of the $O^1H^1\cdots O^2H^2$ and $O^4H^4\cdots O^3H^3$ hydrogen-bonding interactions.

One should mention that the interaction of the γ-$[(SiO_4)W_{10}O_{32}H_4]^{4-}$ unit with the countercations, such as tetramethylammonium reported in the experiment,[17] could change its calculated geometrical parameters. A study elucidating the effect of the countercations, as well as of solvent molecules, on the structures and energetics of the polyoxometalates is in progress and will be reported elsewhere.

IV. Conclusions

From the results presented above, we can draw the following conclusions:

(1) The B3LYP/Lan2dz + d(Si) approach adequately describes the geometries of the M_2-γ-Keggin POMs, as well as lacunary POMs.

(2) The full and medium geometrical models are the best for investigating M_2-γ-Keggin POMs. The small model should be used with great caution.

(3) The energy gap between the lower-lying electronic states of the Fe_2-γ-Keggin POM is found to be reasonably described by the full and medium sized models used in this paper.

(4) The structure of the tetra-protonated form of the lacunary POM, γ-$[(SiO_4)W_{10}O_{32}H_4]^{4-}$, should be formulated as γ-$[(SiO_4)W_{10}O_{28}(OH)_4]^{4-}$ with four terminal hydroxo ligands, rather than as γ-$[(SiO_4)W_{10}O_{30}(H_2O)_2]^{4-}$ with two aqua and two oxo(terminal) ligands. The observed and calculated asymmetry in the W−O(terminal) bond distances of γ-$[(SiO_4)W_{10}O_{32}H_4]^{4-}$ can be explained in terms of the existence of $O^1H^1\cdots O^2H^2$ and $O^4H^4\cdots O^3H^3$ hydrogen-bonding interactions.

Acknowledgment. The present research was supported by a grant from the U.S. Department of Energy (DE-FG0203ER15461). Acknowledgment is made to the Cherry L. Emerson Center of Emory University for the use of its resources, as well as to EMSL Grand Challenge Grant (gc3568) at Pacific Northwest National Laboratory for generous support of computer time and partial use of their NW-Chem software.

IC0490674